4

Active Filters

Rolf Schaumann
Department of Electrical and Computer Engineering, Portland State University, Portland, Oregon, USA

4.1 Introduction

Electrical filters are circuits designed to shape the magnitude and/or phase spectrum of an input signal to generate a desired response at the output. Thus, a frequency range can be defined as the **passband** where the input signal should be transmitted through the filter undistorted and unattenuated (or possibly amplified); **stopbands** require transmission to be blocked or the signal to be at least highly attenuated. In the frequency domain, the transmission characteristic is described by the **transfer function**:

$$T(s) = \frac{V_{\text{out}}}{V_{\text{in}}} = \frac{N_m(s)}{D_n(s)} = \frac{b_m s^m + b_{m-1}s^{m-1} + \cdots + b_1 s + b_0}{s^n + a_{n-1}s^{n-1} + \cdots + a_1 s + a_0}. \quad (4.1)$$

The nth-order function $T(s)$ is a ratio of two polynomials in frequency $s = j\omega$. In a passband, the transfer function should be approximately a constant, typically unity (i.e., $|T(j\omega)| \approx 1$), so that the attenuation is $\alpha = -20\log|T(j\omega)| \approx 0\,\text{dB}$. In the stopband, we need $|T(j\omega)| << 1$ so that the attenuation α is large, say $\alpha = 60\,\text{dB}$ for $|T(j\omega)| = 0.001$. $N_m(s)$ and $D_n(s)$, with $n \geq m$, are chosen so that the attenuation specification is as prescribed (Schaumann and van Valkenburg, 2001). All numerator coefficients b_j are real and, for stable circuits, all denominator coefficients a_i are positive. As a realistic example, consider a low-pass filter. Its passband attenuation must vary by no more than 0.1 dB in $0 \leq f \leq 21\,\text{kHz}$; the stopband attenuation must be at least 22 dB in $f \geq 26\,\text{kHz}$, and it is required to have 12.5-dB low-frequency gain. These requirements call for the fifth-order elliptic function (Zverev, 1967):

$$T(s) = \frac{9.04(s^4 + 2,718.9s^2 + 1,591,230.9)}{s^5 + 40.92s^4 + 897.18s^3 + 28,513.8s^2 + 400,103.6s + 3,411,458.7}, \quad (4.2)$$

where the frequency is normalized with respect to 1 krad/s. A sketch of the function is shown in Figure 4.1.

The denominator polynomial of $T(s)$ in equation 4.1 can be factored to display its n roots, the **poles**, which are restricted to the left half of the s plane. Assuming that n is even and keeping conjugate complex terms together, the factored expression is as written here:

$$D_n(s) = s^n + a_{n-1}s^{n-1} + \cdots + a_1 s + a_0 = \prod_{i=1}^{n/2}\left(s^2 + s\frac{\omega_{0i}}{Q_i} + \omega_{0i}^2\right). \quad (4.3)$$

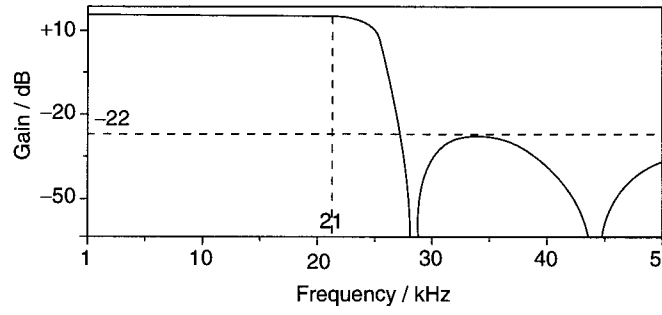

FIGURE 4.1 Sketch of the Elliptic Low-Pass Filter Characteristic of Equation 4.2

The variable ω_{0t} represents the pole frequencies, and Q_i refers to the pole quality factors of the conjugate complex pole pairs:

$$p_i, p_i^* = -\omega_{0i}\left(\frac{1}{2Q_i} \pm j\sqrt{1-\frac{1}{4Q_i^2}}\right). \tag{4.4}$$

Note that $Q_i > 0$ for stable circuits with poles in the left half of the s plane and that the poles are complex if $Q_i > 1/2$. If n is odd, the product in equation 4.3 contains one first-order term. Similarly, $N_m(s)$ may be factored to give:

$$\begin{aligned} N_m(S) &= b_m s^m + b_{m-1}s^{m-1} + \cdots + b_1 s + b_0 \\ &= \prod_{j=1}^{m/2}(k_{2j}s^2 + k_{1j}s + k_{0j}), \end{aligned} \tag{4.5}$$

where a first-order term (i.e., $k_{2j} = 0$) will appear if m is odd. The roots of $N_m(s)$ are the **transmission zeros** of $T(s)$ and may lie anywhere in the s plane. Thus, the signs of k_{ij} are unrestricted. For example, $k_{1j} = 0$ for transmission zeros on the $j\omega$ axis. Assuming now $m = n$, the following is true:

$$\begin{aligned} T(s) = \frac{N_m(s)}{D_n(s)} &= \frac{\prod_{j=1}^{m/2}(k_{2j}s^2 + k_{1j}s + k_{0j})}{\prod_{i=1}^{n/2}(s^2 + s\omega_{0i}/Q_i + \omega_{0i}^2)} \\ &= \prod_{i=1}^{n/2}\frac{k_{2i}s^2 + k_{1i}s + k_{0i}}{s^2 + s\omega_{0i}/Q_i + \omega_{0i}^2} = \prod_{i=1}^{n/2} T_i(s). \end{aligned} \tag{4.6}$$

In case $m < n$, the numerator of equation 4.6 has $(n-m)/2$ factors equal to unity. The objective is now to design filter circuits that realize this function.

For the fifth-order example function in equation 4.2, factoring results in three sections:

$$\begin{aligned} T(s) &= T_1(s)T_2(s)T_3(s) \\ &= \frac{38.73}{s+16.8}\,\frac{0.498(s^2+29.2^2)}{s^2+19.4s+20.01^2}\,\frac{0.526(s^2+43.2^2)}{s^2+4.72s+22.52^2}, \end{aligned} \tag{4.7}$$

where the gain constants are determined to equalize[1] the signal level throughout the filter and to realize a 12.5-dB passband gain. Obtained were two second-order low-pass functions, each with a finite transmission zero (at 29.2 kHz and at 43.2 kHz), and one first-order low-pass.

[1] Since the signal level that an op-amp can handle without distortion is finite and the circuits generate noise, dynamic range is limited. To maximize dynamic range, the first- and second-order blocks in equation 4.7 are cascaded in Figure 4.4 in the order of increasing Q values, and the gain constants are chosen such that the signal level throughout the cascade stays constant.

4.2 Realization Methods

Typically, filter applications have sharp transitions between passbands and stopbands and have complex poles close to the $j\omega$ axis; that is, their quality factors, Q_i, are large. The realization of such high-Q poles requires circuit impedances that change their values with frequency very rapidly. This problem has been solved traditionally with **resonance**: the implementation requires inductors, L, and capacitors, C, because RC circuits have poles only on the negative real axis in the s-plane where $Q \leq 1/2$. Because inductors are large and bulky, LC circuits cannot easily be miniaturized (except at the highest frequencies) so that other approaches are needed for filters in modern communications and controls systems. A popular and widely used solution that avoids bulky inductors makes use of the fact that complex high-Q pole pairs can be implemented by combining RC circuits with **gain**. Gain in active circuits is most commonly provided by the operational amplifier, the op-amp, or sometimes by the operational transconductance amplifier (OTA). It is very easy to see that complex poles can indeed be obtained from **active RC** circuits. Consider an inverting lossy integrator, as shown in Figure 4.2(A), and a noninverting lossless (ideal) integrator, as shown in Figure 4.2(B). Using conductances, $G = 1/R$, and assuming the op-amps are ideal, the lossy and lossless integrators, respectively, realize the functions:

$$\frac{V_B}{V_1} = -\frac{G}{sC+G_q} = -\frac{1}{s\tau+q}$$

and

$$\frac{V_L}{V_B} = \frac{G}{sC} = \frac{1}{s\tau}. \tag{4.8}$$

The integrator time constant is $\tau = RC$ and the loss term is $q = R/R_q$. If these two integrators are connected in a two-integrator loop shown in Figure 4.3, the function realized is:

$$V_L = \left(-\frac{1}{s\tau+q}\times\frac{1}{s\tau}\right)(KV_{in}+V_L)$$

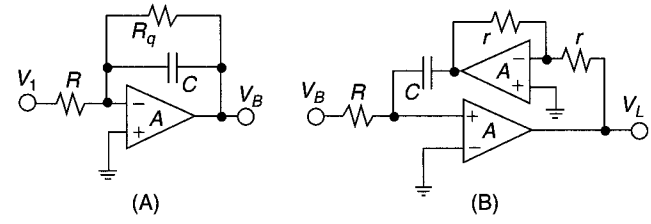

FIGURE 4.2 Integrators (A) Lossy Inverting Integrator (B) Lossless Noninverting Integrator

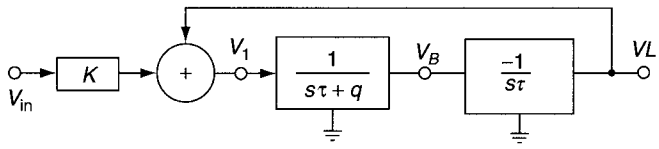

FIGURE 4.3 Two-Integrator Loop Realizing a Second-Order Active Filter (Note that one of the blocks in inverting so that the loop gain is negative for stability).

or

$$\frac{V_L}{V_{\text{in}}} = -\frac{K}{s^2\tau^2 + s\tau q + 1}. \tag{4.9a}$$

If we compare the denominator of equation 4.9a with a pole-pair factor in equation 4.3, we notice that the pole frequency is implemented as $\omega_{0i} = 1/\tau = 1/(RC)$, and the pole quality factor is $Q_i = 1/q = R_q/R$. Clearly, we may choose R_q larger than R, so that $Q_i > 1$ and the poles are complex. In addition, a band-pass function is realized at the output V_B because according to Figure 4.3, we have $V_B = s\tau V_L$ to give with equation 4.9a:

$$\frac{V_B}{V_{\text{in}}} = -\frac{s\tau K}{s^2\tau^2 + s\tau q + 1}. \tag{4.9b}$$

After this demonstration that inductors are not required for high-Q filters, we need to consider next how to implement practical high-order active filters as described in equation 4.6. We shall discuss the two methods that are widely used in practice: **cascade design** and **ladder simulation.**

When analyzing the circuits in Figure 4.2 to obtain equation 4.8, we did assume **ideal op-amps** with infinite gain A and infinite bandwidth. The designer is cautioned to investigate very carefully the validity of such an idealized model. Filters designed with ideal op-amps will normally not function correctly except at the lowest frequencies and for moderate values of Q. A more appropriate op-amp model that is adequate for most filter applications uses the finite and frequency-dependent gain $A(s)$:

$$A(s) = \frac{\omega_i}{s + \sigma} \approx \frac{\omega}{s}. \tag{4.10}$$

That is, the op-amp is modeled as an integrator. The op-amp's −3-dB frequency, σ, (typically less than 100 Hz), can be neglected for most filter applications as is indicated on the right-hand side of equation 4.10. The ω_t is the op-amp's gain-bandwidth product (greater than 1 MHz). To achieve predictable performance, the operating frequencies of active filters designed with op-amps should normally not exceed about $0.1\omega_t$. The Ackerberg-Mossberg and *GIC* second-order sections discussed below have been shown to be optimally insensitive to the finite value of ω and to behave very well even when designed with real operational amplifiers.

4.2.1 Cascade Design

In cascade design, a transfer function is factored into low-order blocks or sections as indicated in equation 4.6. The low-order blocks are then connected in a chain, or are **cascaded** as in Figure 4.4, such that the individual transfer functions multiply:

$$\begin{aligned}\frac{V_{\text{out}}}{V_{\text{in}}} &= \frac{V_1}{V_{\text{in}}} \times \frac{V_2}{V_1} \times \frac{V_3}{V_2} \times \cdots \times \frac{V_{\text{out}}}{V_{n/2-1}} \\ &= T_1 T_2 T_3 \cdots T_{n/2-1} = \prod_{i=1}^{n/2} T_i,\end{aligned} \tag{4.11}$$

as required by equation 4.6. This simple process is valid provided that the individual sections do not interact. Specifically, section T_{i+1} must not load section T_i. In active filters, this is generally not a problem because the output of a filter section is taken from an op-amp output. The output impedance of an op-amp is low, ideally zero, and therefore can drive the next stage in the cascade configuration without loading effects. A major advantage of cascade design is that transfer functions with zeros anywhere in the s-plane can be obtained. Thus, arbitrary transfer functions can be implemented. Ladder simulations have somewhat lower passband sensitivities to component tolerances, but their transmission zeros are restricted to the $j\omega$ axis.

To build a cascade filter, we need to identify suitable second-order (and first-order, if they are present) filter sections that realize the factors in equation 4.6. The first- and second-order functions, respectively, are the following:

$$T_1(s) = \frac{as + b}{s + \sigma} \tag{4.12a}$$

and

$$T_2(s) = \frac{k_2 s^2 + k_1 s + k_0}{s^2 + s\omega_0/Q + \omega_0^2}. \tag{4.12b}$$

In the first-order function, T_1, a and b may be positive, negative, or zero, but σ must be positive. Similarly, in the second-order function, the coefficients k_1 can be positive, negative, or zero, depending on where T_2 is to have transmission zeros. For example, T_2 can realize a low-pass ($k_2 = k_1 = 0$), a high-pass ($k_1 = k_0 = 0$), a band-pass ($k_2 = k_0 = 0$), a band-rejection or

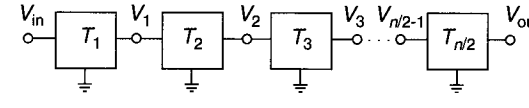

FIGURE 4.4 Realizing a High-Order Filter as a Cascade Connection of Low-Order Sections

"notch" filter ($k_1 = 0$) with transmission zeros at $\pm j\sqrt{k_0/k_2}$, and an all-pass or delay equalizer ($k_2 = 1, k_0 = \omega_0^2, k_1 = -\omega_0/Q$). An example for the choice of coefficients of a first-order low-pass and two second-order notch circuits was presented in equation 4.7.

First-Order Filter Sections

The function T_1 in equation 4.12a is written as:

$$T_1(s) = \frac{V_2}{V_1} = -\frac{sC_1 + G_1}{sC_2 + G_2} = -\frac{(C_1/C_2)s + 1/(C_2R_1)}{s + 1/(C_2R_2)}, \quad (4.13)$$

from which we can identify:

$$a = \frac{C_1}{C_2}, \quad b = \frac{1}{C_2R_1}, \quad \sigma = \frac{1}{C_2R_2} \quad (4.14)$$

Note, however, that the circuit is inverting and causes a (normally unimportant) phase shift of 180°. The example of the first-order low-pass in equation 4.7 is realized by the circuit in Figure 4.5 with $C_1 = 0$, $R_2 = 2.31R_1$, and $C_2R_2 = 1/(16.8\,\text{krad/s})$. The components can be determined if C_2 is chosen (e.g., as 1 nF). We obtain $R_1 = 4.10\,\text{k}\Omega$ and $R_2 = 9.47\,\text{k}\Omega$.

Often, a zero in the right half of the plane is needed (i.e., $b/a < 0$). For this case, the circuit in Figure 4.5(B) can be used. It realizes, with $\sigma = 1/(RC)$:

$$T_1(s) = \frac{V_2}{V_1} = \frac{s - (R_F/R)\sigma}{s + \sigma}. \quad (4.15)$$

For $R_F = R$, the circuit in Figure 4.5(B) realizes a first-order all-pass function that changes the phase but not the magnitude of an input signal.

Second-Order Filter Sections. The literature on active filters contains a large number of second-order sections, the so-called **biquads**, which can be used to realize T_2 in equation 4.12b. Among those, we shall only present three circuits that have proven themselves in practice because of their versatility and their low sensitivities to component tolerances and to finite ω_t-values of the op-amps. The first is the four-amplifier **Ackerberg-Mossberg biquad** that may be called a universal filter because it can implement any kind of second-order transfer function. Then we shall consider the more restrictive two-amplifier **GIC section** that is derived from an **RLC** prototype and has been found to have excellent performance. Finally, we shall present the single-amplifier **Delyiannis-Friend biquad**, which is more sensitive than the previous two circuits but may be used in applications where considerations of cost and power consumption are critical.

The Ackerberg-Mossberg Biquad. The Ackerberg-Mossberg biquad is a direct implementation of the two-integrator loop in Figure 4.3 with the two integrators of Figure 4.2. Adding further a summer that combines all amplifier output voltages weighted by different coefficients, we obtain the circuit in Figure 4.6. Using routine analysis,[2] we can derive the transfer function of the circuit as:

$$\frac{V_{\text{out}}}{V_{\text{in}}} = -\frac{as^2 + s\omega_0/Q[a - b(kQ)] + \omega_0^2[a - (c - d)k]}{s^2 + s\omega_0/Q + \omega_0^2}. \quad (4.16)$$

The parameters a, b, c, d, and k, and the quality factor Q are given by the resistors shown in Figure 4.6, and the pole frequency equals $\omega_0 = 1/(RC)$. If we compare the function with

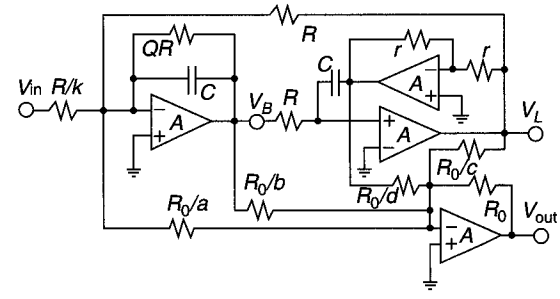

FIGURE 4.6 The Ackerberg-Mossberg Biquad with Output Summer

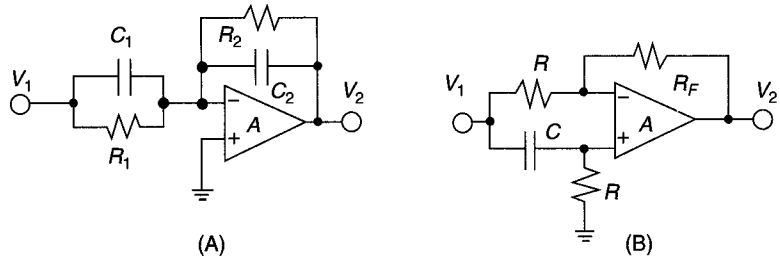

FIGURE 4.5 Active Circuits Realizing the Bilinear Function. (A) Realization for Equation 4.13. (B) Realization for Equation 4.15.

[2] The op-amps are again assumed ideal. This assumption is justified because the combination of the two particular integrators in the Ackerberg-Mossberg circuit causes cancellation of most errors induced by finite ω_t.

T_2 in equation 4.12b, it becomes apparent that an arbitrary set of numerator coefficients can be realized by the Ackerberg-Mossberg circuit. For example, a notch filter with a transmission zero on the $j\omega$ axis requires that $a = bkQ$ by equation 4.16. Notice that the general configuration with the summer is not required for low-pass and band-pass functions: a low-pass function is obtained directly at the output V_L and a band-pass at V_B as we saw in equations 4.9a and 4.9b.

As a design exercise, let us realize T_2 and T_3 in our example function in equation 4.7. We equate formula 4.16 with:

$$T_2(s) = \frac{0.498(s^2 + 29.2^2)}{s^2 + 19.4s + 20.01^2}$$

and

$$T_3(s) = \frac{0.526(s^2 + 43.2^2)}{s^2 + 4.72s + 22.52^2}.$$

With $\omega_{02} = 20.01$ (normalized) and $Q_2 = 20.01/19.4 = 1.03$ for T_2, we find by comparing coefficients that $a = 0.498$, $b = a/(kQ) = 0.498/(1.03 \cdot k)$, and $a - (c - d)k = 1.06$. Choosing for convenience, $k = 1$ and $c = 0$ yields $b = 0.483$ and $d = 0.562$. The choice of $C = 1\,\text{nF}$ leads to $R = 7.95\,\text{k}\Omega$. The value r for the inverter is uncritical, as is R_0; let us pick $r = R_0 = 5\,\text{k}\Omega$; the remaining resistor values are then determined. Similarly, we have for T_3 $\omega_{03} = 22.52$ (normalized) and $Q_3 = 4.77$. We choose again $k = 1$ and $c = 0$ to get $a = 0.526$, $b = a/Q = 0.118$, and $d = 1.41$. The choice of $C = 1\,\text{nF}$ results in $R = 7.07\,\text{k}\Omega$, and $r = R_o = 5\,\text{k}\Omega$ settles the remaining resistor values. If these two second-order sections and the first-order block determined earlier are cascaded according to Figure 4.4, the resulting filter realizes the prescribed function of equation 4.2.

The GIC Biquad A very successful second-order filter is based on the RLC band-pass circuit in Figure 4.7(A) that realizes the following:

$$\frac{V_{\text{out}}}{V_{\text{in}}} = \frac{G}{G + sC + 1/(sL)} = \frac{sG/C}{s^2 + sG/C + 1/(LC)}. \quad (4.17)$$

Since inductors have to be avoided, circuits that use only capacitors, resistors, and gain were developed whose input impedance looks inductive. The concept is shown in Figure 4.7(B) where the box labeled GIC is used to convert the resistor R_L to the inductive impedance Z_L. The **general impedance converter (GIC)** generates an input impedance as $Z_L = sTR_L$, where T is a time constant. For the inductor L in the RLC circuit, we then can substitute a GIC loaded by a resistor $R_L = L/T$.

One way to develop a GIC is to construct a circuit that satisfies the following two-port equations (refer to Figure 4.7(B)):

$$V_1 = V_2, \quad I_1 = I_2/(sT). \quad (4.18)$$

In that case, we have:

$$Z_L = \frac{V_1}{I_1} = sT\frac{V_2}{I_2} = sTR_L, \quad (4.19)$$

exactly as desired. A circuit that accomplishes this feat is shown in the dashed box in Figure 4.7(C). Routine analysis yields $V_2 = V_1$ and $I_2 = s(C_2R_1R_3/R_4)I_1 = sTI_1$ to give the inductive impedance:

$$Z_L(s) = \frac{V_1}{I_1} = s\left(C_2\frac{R_1R_3}{R_4}\right)R_L = sTR_L. \quad (4.20)$$

Normally one chooses in the GIC band-pass filter identical capacitors to save costs: $C = C_2$. Further, it can be shown that the best choice of resistor values (to make the simulated inductor optimally insensitive to the finite gain-bandwidth product, ω_t, of the op-amps) is the following:

$$R_1 = R_3 = R_4 = R_L = 1/(\omega_0 C_2), \quad (4.21)$$

where ω_0 is a frequency that is critical for the application, such as the center frequency in our band-pass case of Figure 4.7 or the passband corner in a low-pass filter. The simulated inductor is then equal to $L = C_2R_1^2$. Finally, the design is completed by choosing $R = QR_1$ to determine the quality factor.

A further small problem exists because the output voltage in the RLC circuit of Figure 4.7(A) is taken at the capacitor node. In the active circuit, this node (V_1 in Figure 4.7(C)), is not an op-amp output and may not be loaded without disturbing the filter parameters. A solution is readily obtained. The voltage V_{out} in Figure 4.7(C) is evidently proportional to V_1 because $V_2 = V_1$: $V_{\text{out}}/V_1 = 1 + R_4/R_L = 2$. Therefore,

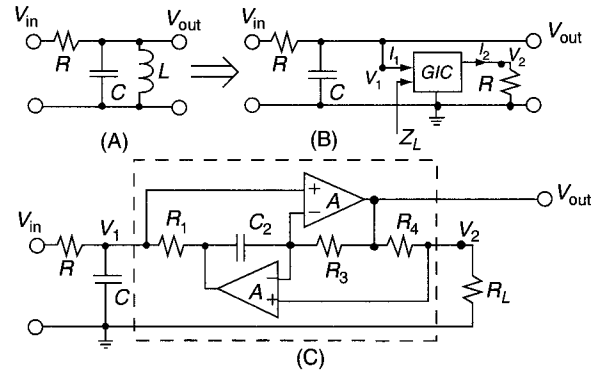

FIGURE 4.7 (A) RLC Prototype Band-Pass Filter (B) Inductor Simulation with a General Impedance Converter (C) The Final GIC Band-Pass Filter with *GIC* Enclosed

we may take the filter output at V_{out} for a preset gain of $V_{out}/V_1 = 2$. The band-pass transfer function realized by the circuit is then

$$\frac{V_{out}}{V_{in}} = \frac{2s/(CR)}{s^2 + s/(CR) + 1/(C^2R_1^2)} = \frac{2s\omega_0/Q}{s^2 + s\omega_0/Q + 1/\omega_0^2}. \quad (4.22)$$

Transfer functions other than a band-pass can also be obtained by generating additional inputs to the GIC band-pass kernel in Figure 4.7(c).

The Single-Amplifier Biquad On occasion, considerations of cost and power consumption necessitate using a single op-amp per second-order section. In that case, the single-amplifier biquad (SAB) of Figure 4.8 may be used. Depending on the choice of components, the circuit can realize a variety of, but not all, different transfer functions. The function realized by this circuit is written as:

$$T(s) = b\frac{s^2 + s\frac{\omega_0}{Q_0}\left[1 + 2Q_0^2\left(1 - \frac{a/b}{1-K}\right)\right] + \omega_0^2}{s^2 + s\frac{\omega_0}{Q_0}\left(1 - 2Q_0^2\frac{K}{1-K}\right) + \omega_0^2}. \quad (4.23)$$

The pole frequency equals $\omega_0 = 1/\left(C\sqrt{R_1R_2}\right)$. To optimize the performance, $R_2 = 9R_1$ and $Q_0 = 1.5$ are chosen. The realized pole quality factor then becomes:

$$Q = \frac{1.5}{1 - 4.5K/(1-K)}. \quad (4.24)$$

Evidently, Q is very sensitive to the tap position, K, of the resistor R and must be adjusted carefully. This filter is particularly useful for building low-Q gain or delay equalizers to improve the performance of a transmission channel.

4.2.2 Realization of Ladder Simulations

Because of their low passband sensitivity to component tolerances, LC ladders have been found to be among the best performing filters that can be built. Therefore, a tremendous effort has gone into designing active filters that retain the excellent performance of LC ladders without having to build and use inductors. A ladder filter consists of alternating series and shunt immittance branches that, as the name implies, are lossless and contain only inductors and capacitors. A typical structure of an LC ladder is shown in Figure 4.9. The circuit consists of five ladder arms (C_1, $L_2\|C_2$, C_3, $L_4\|C_4$, and C_5) and source and load resistors R_1 and R_2. It can realize the fifth-order low-pass function of equation 4.2 with the transfer behavior sketched in Fig. 2.6.1. The two transmission zeros at 29.2 kHz and 43.2 kHz are realized by the parallel resonance frequencies of $L_2\|C_2$ and $L_4\|C_4$. The question to be addressed is how to implement such a circuit without the use of inductors.

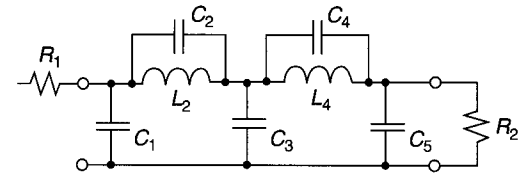

FIGURE 4.9 Typical (Low-Pass) LC Ladder Filter: This circuit is of the form required to realize the transfer function of equation 4.2 with the attenuation curve of Figure 4.1.

The problem is attacked in two different ways. The **element replacement method** eliminates the inductors by electronic circuits whose input impedance is inductive over the relevant frequency range. We encountered this method in Figure 4.7, where the need for an inductor was avoided when L was replaced by a GIC terminated in a resistor. The **method of operational simulation** makes use of the fact that inductors and capacitors fundamentally perform the function of integration, 1/s. Specifically, the voltage V across an inductor generates the current $I = V/(sL)$, and the current I through a capacitor is integrated to produce the voltage $V = I/(sC)$. Thus, we should need only to employ electronic integrators, as in Figure 4.2, to arrive at an inductorless simulation of an LC ladder.

The Element-Replacement Method

In a complete analogy to the GIC biquad discussed earlier, we now create the inductive impedance Z_L at the input of a GIC that is loaded by a resistor R [see Figure 4.10(A)]. The GIC circuit used here is shown in Figure 4.10(B). Notice that compared to Figure 4.7(C), we interchanged the capacitor and the resistor in positions 2 and 4. From equation 4.20, the time constant equals $T = C_4R_1R_3/R_2$. This change is immaterial as far as Z_L is concerned, but the selection is optimal for this case. Note that we have attached the label $1{:}sT$ to the GIC boxes to help us keep track of their orientation in the following development: the sT side faces the resistive load. It was shown in equation 4.18 that the GIC implements the two-port equations for the element choice in Figure 4.10(B):

$$V_1 = V_2,\ I_2 = C_4\frac{R_1R_3}{R_2} = sTI_1. \quad (4.25)$$

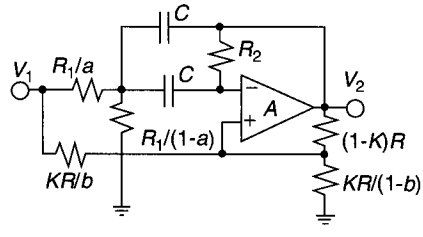

FIGURE 4.8 The Delyiannis-Friend Single-Amplifier Biquad (SAB)

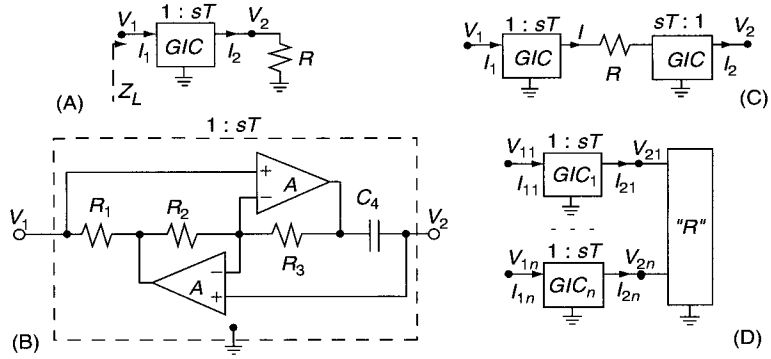

FIGURE 4.10 Circuits for the Element-Replacement Method

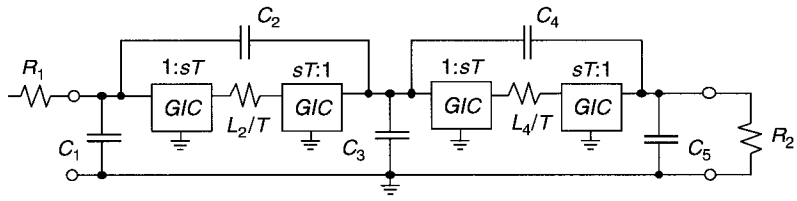

FIGURE 4.11 Inductors in the LC Ladder of Figure 4.9: The inductors simulated by resistors of value $L_i/T, i = 2, 4$, which are embedded between two GICs.

Consequently, the input impedance of the circuit in Figure 4.10(A) is that of a grounded inductor $L = TR$:

$$Z_L = \frac{V_1}{I_1} = sT\frac{V_2}{I_2} = sTR = sL, \tag{4.26}$$

and this scheme can be used to replace any **grounded** inductor in a filter. A **floating** inductor can be implemented by using two GICs as shown in Figure 4.10(C). It is a simple extension of the circuit in Figure 2.10(A), obtained by noting that the resistor is grounded as in Figure 4.10(A) for $V_2 = 0$, according to equation 4.25, input and output voltages of the GIC are the same. The same is true for $V_1 = 0$. Because the voltage $\Delta V = V_1 - V_2$ appears across the series resistor R, we have $I = (V_1 - V_2)/R$. Observing the orientation of the two GIC boxes, we find further $I_2 = I/(sT)$ and:

$$I_1 = I_2 = \frac{V_1 - V_2}{sTR} = \frac{V_1 - V_2}{sL}. \tag{4.27}$$

Evidently, this equation describes a floating inductor of value $L = TR$. This method affords us a simple way to implement floating inductors L by embedding resistors of value L/T between two GICs. Specifically, for the filter in Figure 4.9, we obtain the circuit in Figure 4.11.

We still remark that this method is relatively expensive in requiring two GICs (four op-amps) for each floating inductor and one GIC (two op-amps) for each grounded inductor. A simplification is obtained by the circuit illustrated in Figure 4.10(D). We have shown a resistive network R that has a $1{:}sT$ GIC inserted in each input lead. The network R is described by the equation:

$$\mathbf{V}_{2k} = \mathbf{R}\mathbf{I}_{2k}, \tag{4.28}$$

where $\mathbf{V}_{2k}$ and $\mathbf{I}_{2k}$ are the vectors of the input voltages and currents, respectively, identified in Figure 4.10(D) and $\mathbf{R}$ is the resistance matrix describing the network and linking the two vectors. By equation 4.25, we have from the GICs the relationships $\mathbf{V}_{1k} = \mathbf{V}_{2k}$ and $\mathbf{I}_{2k} = sT\mathbf{I}_{1k}$ so that with equation 4.28, we obtain the result:

$$\mathbf{V}_{1k} = \mathbf{V}_{2k} = \mathbf{R}\mathbf{I}_{2k} = \mathbf{R}sT\mathbf{I}_{1k} = sT\mathbf{R}\mathbf{I}_{1k} \tag{4.29}$$

or

$$\mathbf{V}_{1k} = sT\mathbf{R}\mathbf{I}_{1k} = s\mathbf{L}\mathbf{I}_{1k}. \tag{4.30}$$

This equation implies that a resistive network embedded in GICs appears like an inductive network **of the same topology** with the inductance matrix $\mathbf{L} = T\mathbf{R}$, that is, each inductor L is replaced by a resistor of value L/T. This procedure is the **Gorski-Popiel** method. Its significance is that it permits complete inductive subnetworks to be replaced by resistive subnetworks embedded in GICs, rather than requiring each inductor to be treated separately. Depending on the topology

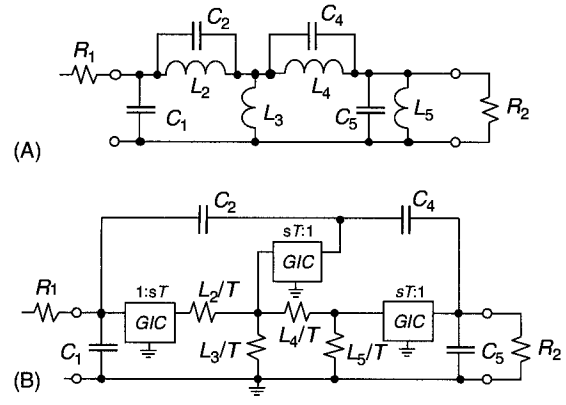

FIGURE 4.12 (A) *LC* Band-Pass Ladder (B) Realization by Gorski-Popiel's Element-Replacement Method

of the *LC* ladder, Gorski-Popiel's method may save a considerable number of GICs, resulting in reduced cost, power consumption, and noise. The simulation of the band-pass ladder in Figure 4.12(A) provides an example for the efficiencies afforded by Gorski-Popiel's procedure. Converting each inductor individually would require six GICs, whereas identifying first the inductive subnetwork consisting of all four inductors leads to only three GICs for the active simulation of the ladder shown in Figure 4.12(B).

Operational Simulation or Signal-Flow Graph Implementation of LC Ladders

As mentioned earlier, in the SFG simulation of an LC ladder filter, each inductor and capacitor are interpreted as signal-flow integrators that can be implemented by an RC/op-amp circuit. The method is completely general in that it permits arbitrary ladder arms to be realized, but in this chapter, we shall illustrate the procedure only on low-pass ladders.

Consider the general section of a ladder shown in Figure 4.13(A). It can be represented by the equations:

$$V_1 = \frac{I_0 - I_2}{Y_1},\quad V_3 = \frac{I_2 - I_4}{Y_3},\quad V_5 = \frac{I_4 - I_6}{Y_5}. \tag{4.31a}$$

$$I_2 = \frac{V_1 - V_3}{Z_2},\quad I_4 = \frac{V_3 - V_5}{Z_4}. \tag{4.31b}$$

For example, in all-pole low-pass filters, all branches Y_i and Z_j are single capacitors and inductors, respectively, so that the five expressions in equations 4.31(A) and 4.31(B) represent integration. Generally, however, Y_i and Z_j may be arbitrary LC immittances. Equations 4.31(A) and 4.31(B) indicate that differences of voltages and currents that need to be formed, which requires more complicated circuitry than simple summing. To achieve operation with only summers, we recast equations 4.31(A) and 4.31(B) as follows by introducing a number of multiplications with (-1):

$$V_1 = \frac{I_0 + (-I_2)}{Y_1},$$
$$(-V_3) = \frac{(-I_2) + I_4}{Y_3},\quad V_5 = \frac{I_4 + (-I_6)}{Y_5}. \tag{4.32a}$$

$$(-I_2) = \frac{V_1 + (-V_3)}{-Z_2},\quad I_4 = \frac{(-V_3) + V_5}{-Z_4}. \tag{4.32b}$$

Figure 4.13(B) shows the resulting block diagram.

To be able to sum only voltages, we next convert the currents in equations 4.32(A) and 4.32(B) into voltages. This step is accomplished by multiplying all currents by a scaling resistor R and, simultaneously, by multiplying the admittances by R to obtain so-called "transmittances" $t_Y = 1/(RY)$ or $t_Z = R/Z$ as is shown in equation 4.33:

$$V_1 = \frac{RI_0 + (-RI_2)}{RY_1} \Rightarrow v_1 = t_{Y1}[v_{10} + (-v_{12})].$$
$$(-RI_2) = \frac{V_1 + (-V_3)}{-Z_2/R} \Rightarrow -v_{12} = -t_{Z2}[v_1 + (-v_3)].$$
$$(-V_3) = \frac{(-RI_2) + RI_4}{RY_3} \Rightarrow -v_3 = t_{Y3}[(-v_{12}) + v_{14}]. \tag{4.33}$$
$$RI_4 = \frac{(-V_3) + V_5}{-Z_4/R} \Rightarrow v_{14} = -t_{Z4}[(-v_3) + v_5].$$
$$V_5 = \frac{RI_4 + (-RI_6)}{RY_5} \Rightarrow v_5 = t_{Y5}[v_{14} + (-v_{16})].$$

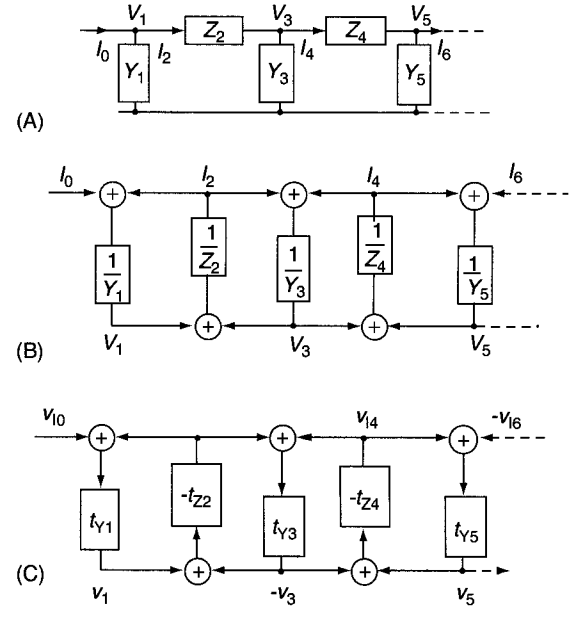

FIGURE 4.13 (A) Section of a General Ladder (B) Signal-Flow Graph Representation for Equation 4.32 (C) Signal-Flow Graph Representation for Equation 4.33

For consistency, we have labeled all voltages, the signals of the SFG implementation, by lowercase symbols and have used the subscripts I, Z, and Y to be reminded of the origin of the dimensionless signals, v, and transmittances, t. Observe that all equations have the same format, $v_k = t_k \times (v_{k-1} + v_{k+1})$, that the signs of all signals are consistent, and (for low-pass ladders) that all t_Z transmittances are inverting and the t_Y transmittances are noninverting integrators: $t_Y = 1/(RY) = 1/(sRC)$, $t_Z = -R/Z = -R/(sL)$. Note also that this process may lead to a normally unimportant sign inversion in the realization. Equations 4.33 are represented by the signal-flow graph in Figure 4.13(C) (Martin and Sedra, 1978). Also observe that inverting and noninverting integrators alternate so that all loops have negative feedback (the loop-gain is negative) and are stable. In low-pass filters, the boxes, together with the summing junctions, form summing integrators that now have to be implemented.

The integrators can be obtained from the circuits n Figure 4.2 by adding a second input. As drawn in Figure 4.13(C), the inverting integrators point upward and the noninverting integrators downward. We used this orientation for the circuits in Figure 4.14. Apart from the sign, both circuits realize the same two-input lossy integrator functions,

$$V_2 = \pm \frac{a_1 V_{11} + a_2 V_{12}}{s\tau + q}, \qquad (4.34)$$

where the minus sign is for the inverting integrator in Figure 4.14(A), and the plus sign for the noninverting integrator in Figure 4.14(B). We used a scaling resistor R_a to define $\tau = C_A R_a$, $q = R_a/R_q$, the gain constants $a_1 = R_a/R_1$, and $a_2 = R_a/R_2$ that multiply the two input voltages V_{11} and V_{12}. These gain constants can be adjusted to maximize the dynamic range of the active filter, but the treatment goes beyond the scope of this chapter. We will for simplicity set $a_1 = a_2 = 1$ by selecting $R_a = R_1 = R_2 = R$ to get $\tau = C_A R$ and $q = R/R_q$. Remember still that the LC ladder is lossless. All *internal* integrators are, therefore, lossless (i.e. $q = 0$, $R_q = \infty$). A finite value for R_q is needed only for the first and last ladder arms where R_q serves to realize source and load resistors.

As an example for the signal-flow graph technique, consider the low-pass ladder in Figure 4.15(A). The component values are $R_S = R_L = 1\text{k}\Omega$, $C_1 = C_3 = 20\,\text{nF}$, and $L_2 = 30\,\text{mH}$. The filter has a flat passband; the 1-dB passband corner is at 9.6 kHz.

The first step in the realization is a Norton source transform to convert the voltage source into a current source, so that the source resistor is placed in parallel to C_1. This transformation removes one mesh from the circuit and simplifies the design as in Figure 4.15(B). Let us write the describing equations to understand how the components in the active circuit are derived from the ladder. Choosing as the scaling resistor R_S, we obtain

$$V_1 = \frac{R_S(V_{in}/R_S) + (-I_L)R_S}{R_S G_S + sC_1 R_S},$$

$$-I_L R_S = \frac{V_1 + (-V_2)}{sL_2/R_S}, \quad -V_2 = \frac{-I_L R_S}{R_S G_L + sC_3 R_S}.$$

These equations need to be compared with those of the integrators, equation 4.34, to determine the element values. Since $C_1 = C_3$ and $R_S = R_L$, the first and last lossy integrators are the same. The comparison yields $C_1 R_S = C_3 R_S = \tau = C_A R_a$, $q_1 = q_3 = G_S/R_S = 1$, $C_2 R_S = \tau_2 = L_2/R_S$, and $q_2 = 0$. If we select[3] $R_a = R_S = 1\,\text{k}\Omega$, we have $C_1 = C_3 = 20\,\text{nF}$ and $C_2 = L_2/R_S^2 = 30\,\text{nF}$. The value of r is unimportant; let us choose $r = 1\,\text{k}\Omega$ so that all resistors have the same value. The final circuit is shown in Figure 4.15(C). Notice that each loop combines the inverting and noninverting integrators, which we used earlier to construct the Ackerberg-Mossberg

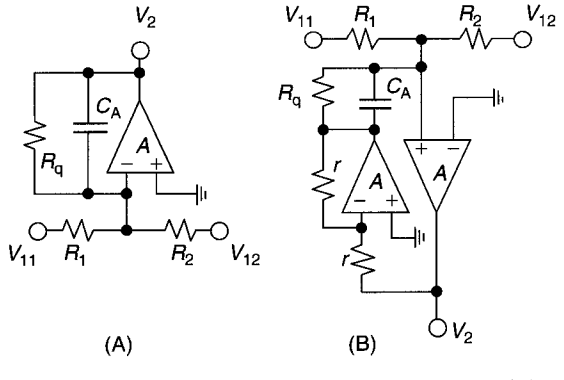

FIGURE 4.14 (A) Inverting Lossy Summing Integrator (B) Noninverting Lossy Summing Integrator

[3] Alternatively, we could choose different resistor values and arrive at identical capacitors.

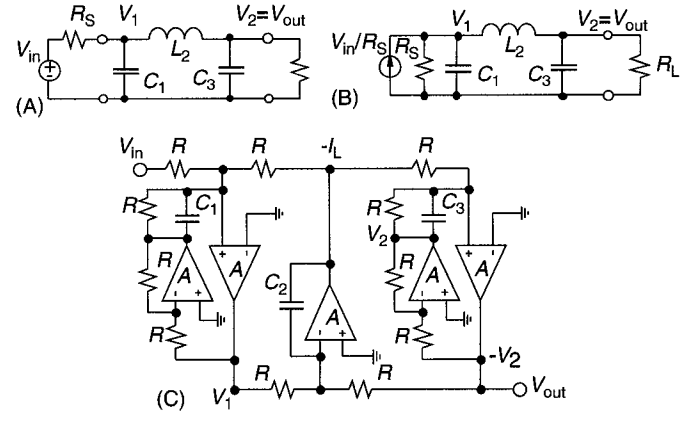

FIGURE 4.15 Realizing a Low-Pass Ladder by the Signal-Flow Graph Technique. (a) The original ladder. (b) Source transformation of the ladder. (c) Final active circuit with $R = 1\,\text{k}\Omega$, $C_1 = C_3 = 20\,\text{nF}$, $C_2 = L_2/R_1^2 = 30\,\text{nF}$.

biquad (see Figure 4.6 without the summer). As a result, we conclude that the performance of this simulated ladder can be expected to be similarly insensitive to the op-amp's finite gain-bandwidth products. Using 741-type op-amps with $f_t \approx 1.5\,\text{MHz}$, the performance of the active circuit is acceptable to over 300 kHz, and the performance of the two circuits in Figure 4.15(A) and 4.15(C) is experimentally indistinguishable until about 90 kHz when the op-amp effects begin to be noticeable. As a final comment, observe that the output V_{out} in the active realization is inverting. If this phase shift of 180° is not acceptable, the output may be taken at the node labeled V_2.

4.2.3 Transconductance-*C* (OTA-*C*) Filters

The finite value of the op-amp's gain-bandwidth product ω_t causes the frequency range of the active filters discussed so far to be limited to approximately $0.1\,\omega_T$. Using inexpensive op-amps in which f_t is of the order 1.5 to 3 MHz is not sufficient because the frequency range is too low for most communications applications. Although relatively economical wideband amplifiers are available with f_t values up to about 100 MHz, a different solution is available that is especially attractive for filter circuits compatible with integrated-circuit (IC) technology. For these cases, gain is not obtained from operational voltage amplifiers but from operational transconductance amplifiers, also labeled OTAs or transconductors. These circuits are voltage-to-current converters characterized by their transconductance parameter g_m that relates the output current to the (normally differential) input voltage:

$$I_{\text{out}} = g_m(V_{\text{in}}^+ - V_{\text{in}}^-). \tag{4.35}$$

Simple transconductors with bandwidths in the GHz range have been designed in standard CMOS technology (Szczepanski *et al.*, 1997); in turn, they permit communication filters to be designed with operating frequencies in the hundreds of megahertz. There are several additional reasons for the popularity of the use of transconductors in filter design. Among them are the small OTA circuitry, the particularly easy filter design techniques that normally permit all OTA cells to be identical, and the compatibility with digital (CMOS) integrated-circuit technology: "OTA-*C*" filters use no resistors.

A small-signal model of the OTA is shown in Figure 4.16(A) including parasitic input and output capacitors (of the order 0.01 to 0.05 pF) and the finite output resistance (of the order of 0.1 to 2 MΩ). We have shown the lower output terminal grounded because for simplicity we shall assume that designs are single-ended for the sake of this discussion. In practice, IC analog circuitry is designed in differential form for better noise immunity, linearity, and dynamic range. Conversion to differential circuitry is straightforward. The customary circuit symbol for the OTA is shown in Figure 4.16(B).

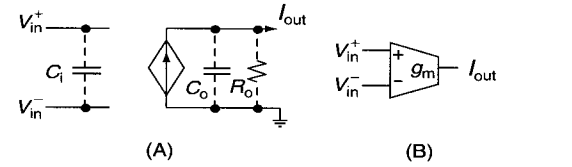

FIGURE 4.16 (A) Small-Signal Model of a Transconductor: $I_{out} = g_m(V_{in}^+ - V_{in}^-)$ (B) Circuit Symbol

Apart from minor differences having to do largely with IC implementation, active filter design with OTAs is the same as filter design with op-amps. As before, we have available the cascade method with first and second-order sections, or we can use ladder simulations. For the latter, it can be shown that element replacement and the signal flow-graph technique lead to identical OTA-*C* filter structures, so only one of the two methods needs to be addressed.

Cascade Design

The only difference between this cascade design method and the one presented earlier (in Section 4.2.1) is the use of only OTAs and capacitors. In this case, the filter sections do not normally have low output impedance, but the input impedance[4] is as a rule very large, so cascading remains possible. General first- and second-order sections are shown in Figure 4.17. The circuit in Figure 4.17(A) realizes the function:

$$T_1(s) = \frac{V_{\text{out}}}{V_{\text{in}}} = \frac{saC + g_{m1}}{sC + g_{m2}}, \tag{4.36}$$

and the second-order section in Figure 4.17(B) implements:

$$T_2(s) = \frac{V_{\text{out}}}{V_{\text{in}}} = \frac{s^2 bC_1C_2 + s(bC_2g_{m2} - aC_1g_{m3}) + g_{m1}g_{m3}}{s^2C_1C_2 + sC_2g_{m2} + g_{m3}g_{m4}}. \tag{4.37}$$

Normally, one selects $g_{m3} = g_{m4} = g_m$; the pole frequency and pole quality factor are then:

$$\omega_0 = \frac{g_m}{\sqrt{C_1C_2}}, \quad Q = \frac{\omega_0 C_1}{g_{m2}} = \sqrt{\frac{C_1}{C_2}}\frac{g_m}{g_{m2}}. \tag{4.38}$$

Since ω_0 is proportional to g_m, which in turn depends on a bias current or voltage, the pole frequency can be tuned by varying the circuit's bias. Automatic electronic tuning techniques have been developed for this purpose. In addition, note that Q, as a dimensionless parameter, is set by ratios of like components

[4] The input of an OTA-*C* filter is normally a parasitic capacitor (≈ 0.05 pF) of a CMOS transistor. Thus, even at 100 MHz, the input impedance is still larger than 30 kΩ. Furthermore, as the topology of the first- and second-order circuits in Figure 4.17 indicates, these input capacitors can be absorbed in the circuit capacitors of the previous filter section.

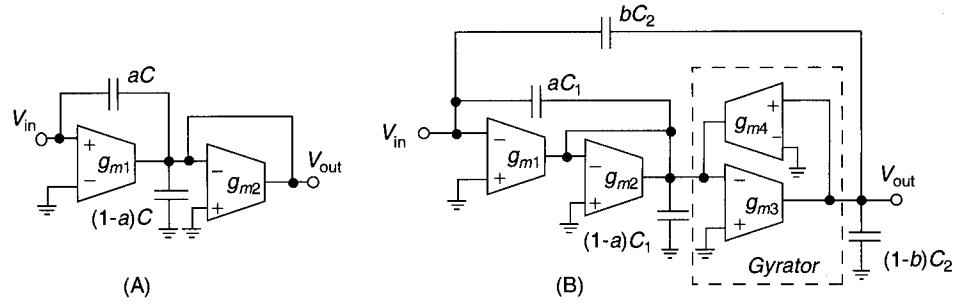

FIGURE 4.17 General OTA-*C* Filter Sections. (A) First-order. (B) Second-order.

and, therefore, is designable quite accurately. Difficulties arise only for large values of Q where parasitic effects can cause large deviations and tuning must be used.

Evidently, a variety of transfer functions can be realized by choice of the components, the coefficients a and b, and the values and signs of the transconductances, g_{mi}. For instance, comparing equation 4.37 with T_2 in equation 4.12 shows that the second-order functions can be realized with arbitrary coefficients. Negative values of g_{mi} are obtained by simply inverting the polarity of their input connections; this must be done with caution, of course, to make certain that the transfer functions' denominator coefficients stay positive.

An interesting observation can be made about the two circuits in Figure 4.17. Notice that all internal nodes of the circuits are connected to a circuit capacitor. This means that the input and output capacitors of all transconductance cells (see Figure 4.16(A)) can be absorbed in a circuit capacitor and do not generate parasitic poles or zeros, which could jeopardize the transfer function. The designer must, however, "predistort" the capacitors by reducing their nominal design values by the sum of all parasitic capacitors appearing at the capacitor nodes. Thus, if a high-frequency design calls for $C = 1.1\,\text{pF}$ and the sum of all relevant parasitics equals 0.2 pF, for example, the circuit should be designed with $C = (1.1 - 0.2)\text{pF} = 0.9\,\text{pF}$. The unavoidable parasitics will restore the effective capacitor to its nominal value of 1.1 pF.

An additional interesting observation can be made related to the structure of the second-order circuit in Figure 4.17(B). We have labeled the circuit in the dashed box a **gyrator**. A gyrator is a circuit whose input impedance is proportional to the reciprocal of the load impedance. Figure 4.18(A) shows the situation for a load capacitor. From this circuit, we derive that the input impedance equals:

$$Z_{in} = \frac{V_1}{I_1} = \frac{1}{g_m^2} sC = s\frac{C}{g_m^2} \Rightarrow sL. \qquad (4.39)$$

That is, it realizes an inductor of value $L = C/g_m^2$. Consequently, we recognize that the second-order OTA-*C* circuit is derived from the passive RLC band-pass stage in Figure 4.7(A) in the same way as the GIC filter in Figure

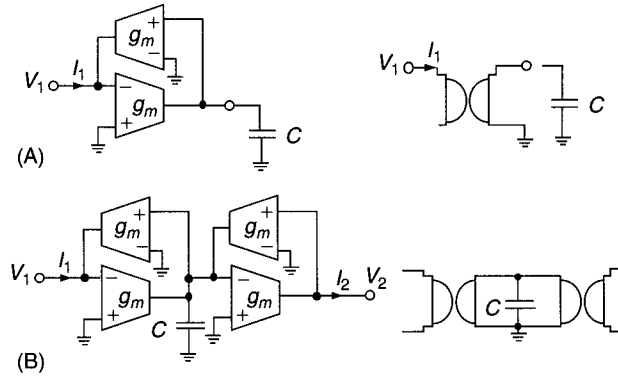

FIGURE 4.18 Capacitor-Loaded Gyrators and their Symbols. (A) Grounded Inductor. (B) Floating Inductor.

4.7(C). Assume[5] for the following discussion that $a = b = 0$ in the circuit in Figure 4.17(B). We observe then that g_{m1} converts the input voltage V_{in} into a current that flows through C_1 and the resistor[6] $1/g_{m2}$. In parallel with the capacitor, C_1, is the inductor $L = C_2/(g_{m3}g_{m4})$. The parallel RLC connection of $1/g_{m2}$, C_1, and $L = C_2/(g_{m3}g_{m4})$ is driven by the current $g_{m1}V_{in}$. The OTA-based grounded inductor can be used in any filter application in the same way as the GIC-based inductor of Figure 4.10(A), except that the OTA-based circuit can be employed at much higher frequencies.

Ladder Simulation

The analogy of the present treatment with the one summarized in Figure 4.10 should let us suspect that floating inductors can be simulated as well by appropriate gyrator connections. Indeed, we only need to connect two gyrators with identical g_m values to a grounded capacitor as shown in Figure 4.18(B) to obtain a floating inductor of value $L = C/g_m^2$. For example,

[5] The fractions a and b of the capacitors C_1 and C_2 are connected to the input to generate a general numerator polynomial from the band-pass core circuit. The method is analogous to the one used in Figure 4.8 for the resistors R_1 and KR.

[6] It is easy to show that a transconductor g_m with its output current fed back to the inverting input terminal acts like a resistor $1/g_m$.

using this approach on the ladder in Figure 4.9 results in the circuit in Figure 4.19, in complete analogy with the GIC circuit in Figure 4.11. Notice that all g_m cells in the simulated ladder are the same, a convenience for matching and design automation. The circuits in Figures 4.11 and 4.19 have identical performance in all respects, except that the useful frequency range of the OTA-based design is much larger. Even when using fast amplifiers with, say, $f_t \approx 100\,\text{MHz}$, the useful operating frequencies of the GIC filter in Figure 4.11 will be less than about 10 MHz, whereas it is not difficult to achieve operation at several 100 MHz with the OTA-based circuit. A signal-flow graph method need not be discussed here because, as we stated, the resulting circuitry is identical to the one obtained with the element replacement method.

The treatment of transconductance-*C* filters in this chapter has necessarily been brief and sketchy. Many topics, in particular the important issue of automatic tuning, could not be addressed for lack of space. The reader interested in this important modern signal processing topic is referred to the literature in the References section for further details.

References

Martin, K. and Sedra, A.S. (1978). Design of signal-flow-graph (SFG) active filters. *IEEE Transactions on Circuits and Systems 25*, 185–195.

Schaumann, R. (1998). Simulating lossless ladders with transconductance-C circuits. *IEEE Transactions on Circuits and Systems* II *45*(3), 407–410.

Schaumann, R., Ghausi, M.S., and Laker, K.R. (1990). *Design of analog filters: Passive, Active RC, and Switched Capacitor.* Englewood Cliffs, NJ: Prentice-Hall.

Szczepanski, S., Jakusz, J., and Schaumann, R. (1997). A linear fully balanced CMOS OTA for VHF filtering applications. *IEEE Transactions on Circuits and Systems*, II *44*, 174–187.

Schaumann, R., and Valkenburg, M.V. (2001). *Modern active filter design.* New York: Oxford University.

Tsividis, Y., and Voorman, J.A. (Eds.). (1993). *Integrated continuous-time filters: Principles, design and implementations.* IEEE Press.

Zverev, A. (1967). *Handbook of filter synthesis.* New York: John Wiley & Sons.